Original Research

Journal of Advanced Veterinary Research
(2026) Volume 16, Issue 3, 387-393

Development of AuNP-based biosensor as an alternative rapid and sensitive method for detection of *Listeria monocytogenes*

Mohamed M.A. Zeinhom[1*], Gamal M. Hassan[1], Mohamed G. Farahat[2], Mostafa A. Tamam[3*], Ahmed M. Korany[1]

[1]*Department of Food Safety and Technology, Faculty of Veterinary Medicine, Beni-Suef University, Beni-Suef 62511, Egypt.*
[2]*Botany and Microbiology Department, Faculty of Science, Cairo University, Cairo, Egypt.*
[3]*Postgraduate at the Department of Food Safety and Technology, Faculty of Veterinary Medicine, Beni-Suef University, Beni-Suef 62511, Egypt.*

ARTICLE INFO

Received: 22 February 2026

Accepted: 31 March 2026

*Correspondence:

Corresponding author: Mostafa A. Tamam
E-mail address: mostafaagamy918@gmail.com

Keywords:

Listeria monocytogenes, PCR, VITEK 2, MALDI-TOF, Milk, Gold nanoparticles

ABSTRACT

Rapid, accurate, and field-deployable detection methods are essential to prevent outbreaks caused by *Listeria monocytogenes* (*L. monocytogenes*), a major foodborne pathogen associated with high morbidity and mortality rates. Conventional detection approaches, including PCR, VITEK-2, and MALDI-TOF/MS, although highly sensitive and specific, typically require 12–24 hours to yield results and depend on sophisticated instrumentation and trained personnel, thereby limiting their on-site applicability. In the present study, we developed a novel colorimetric biosensing platform based on oligonucleotide-functionalized gold nanoparticles (AuNPs) for the rapid, sensitive, and equipment-free detection of *L. monocytogenes*. A total of 200 dairy product samples were analyzed using selective culture media, biochemical assays, automated identification systems, molecular techniques, and the proposed AuNP–oligonucleotide probe biosensor. Of the nine presumptive *L. monocytogenes* isolates, six (66.7%) were confirmed by VITEK-2, MALDI-TOF, PCR, and AuNP-based biosensing. The developed AuNP biosensor demonstrated exceptional analytical performance, achieving a detection limit of 10 pg/µL and 100% specificity in discriminating *L. monocytogenes* from non-target bacterial species. The localized surface plasmon resonance (LSPR) response of the AuNPs exhibited a characteristic absorption peak within the 520–530 nm range, confirming successful target hybridization. This innovative AuNP-based optical biosensing system provides a rapid, accurate, and cost-effective alternative for *L. monocytogenes* detection, bridging the gap between conventional molecular diagnostics and field-based applications. The platform shows significant potential for integration into food safety surveillance programs and clinical diagnostic workflows.

Introduction

Foodborne pathogens pose a major threat to public health and the global food supply chain. Among these, *Listeria monocytogenes* is particularly concerning due to its ability to persist in diverse environments and cause severe illness in vulnerable populations (Ferreira *et al*., 2014; Hoelzer *et al*., 2013). *L. monocytogenes* is a Gram-positive, facultatively anaerobic, non-spore-forming bacterium capable of growth at refrigeration temperatures and survival in extreme conditions, including acidic and alkaline environments (Liu *et al*., 2005; Ferreira *et al*., 2014). Although the incidence of listeriosis is relatively low compared to other foodborne diseases, its hospitalization and fatality rates remain among the highest, reaching up to 30% in immunocompromised individuals and pregnant women (de Noordhout *et al*., 2014; EFSA and ECDC, 2021). The long incubation period (1–70 days) and relatively low infectious dose (10^4–10^7 CFU) further complicate outbreak tracing and clinical management (Buchanan *et al*., 2009; Angelo *et al*., 2017).

Globally, *L. monocytogenes* contamination is frequently associated with ready-to-eat foods and dairy products. In Egypt, isolates have been recovered from 5–26% of raw milk and dairy samples (Abd El-Tawab *et al*., 2015; Tahoun *et al*., 2017), indicating the persistence of this pathogen within the dairy value chain. Similar findings have been reported in other regions, such as Iraq (Abbas and Jaber, 2012) and Iran (Moosavy *et al*., 2014). The capacity of *L. monocytogenes* to form biofilms on equipment surfaces and to tolerate sanitizing agents allows it to survive during processing and storage, leading to potential contamination of finished products (Ferreira *et al*., 2014). Consequently, rapid, sensitive, and reliable detection method for *L. monocytogenes* in dairy products is essential to safeguard public health.

Conventional detection of *L. monocytogenes* relies on selective enrichment and isolation on chromogenic or Oxford agar, followed by biochemical and serological confirmation (Roberts and Greenwood, 2003). While these methods remain the reference standard, they are labor-intensive and time-consuming, typically requiring 3–7 days to yield confirmed results (Rezaei *et al*., 2019).

To overcome these drawbacks, molecular and automated diagnostic systems have been implemented. PCR assays targeting virulence genes such as *hly* and iap enable more rapid identification (Dapgh and Salem, 2022), and real-time PCR has further enhanced sensitivity and quantification capability (Zhang *et al*., 2017). Similarly, automated biochemical identification systems (VITEK-2) and MALDI-TOF MS offer fast species-level confirmation based on metabolic and proteomic fingerprints (Araújo *et al*., 2020; Li *et al*., 2022). However, these tools require advanced infrastructure, skilled personnel, and pure isolates, restricting their utility in low-resource or field settings. Moreover, misidentification, especially confusion between *L. monocytogenes* and *L. innocua*, has been reported in automated systems (De Lappe *et al*., 2014; Pyz-Łukasik *et al*., 2021).

Thus, while culture, PCR, and MALDI-TOF methods remain essential for reference laboratories, their high cost, complexity, and prolonged processing time hinder real-time decision making in food inspection and outbreak control. These constraints underscore the need for rapid, sensitive, and field-deployable detection alternatives that maintain accuracy without dependence on sophisticated instrumentation.

Biosensor technology integrates biological recognition elements with physical transducers to convert biorecognition events into measurable signals. Among the major categories, including electrochemical, piezoelectric, and optical biosensors, optical biosensors have attracted considerable attention for pathogen detection due to their simplicity, high sensitivity, and rapid response (Zhu *et al*., 2017).

Gold nanoparticles (AuNPs) are especially attractive for biosensing applications because of their unique localized surface plasmon resonance (LSPR) properties, ease of surface functionalization, and strong optical

ISSN: 2090-6277/2090-6269/

absorption in the visible range (Yola and Atar, 2014). The LSPR phenomenon arises from collective oscillations of conduction electrons on AuNP surfaces when excited by light, producing a characteristic absorbance peak around 520–530 nm. Upon aggregation, plasmon coupling causes a visible color shift from red to blue, which forms the basis of colorimetric biosensing (Gupta *et al*., 2013).

By modifying AuNP surfaces with thiol-linked oligonucleotides, highly specific DNA hybridization events can be transduced into color changes detectable by eye or a simple spectrophotometer. Such assays have been successfully used for various pathogens, including *Escherichia coli* and *Salmonella enterica* (Wachiralurpan *et al*., 2018; Quintela *et al*., 2019). AuNP-based colorimetric biosensors eliminate the need for sophisticated optical equipment, allowing for point-of-care (POC) or field diagnostics with high specificity and sensitivity. Despite these advantages, few studies have validated AuNP-based sensors for *L. monocytogenes* in complex food matrices. Food components such as proteins, fats, and salts can interfere with probe hybridization or nanoparticle stability. Therefore, developing a robust AuNP-oligonucleotide biosensor that performs reliably in real dairy samples remains a critical gap.

Given the limitations of current diagnostic systems, there is an urgent demand for rapid, accurate, and equipment-free methods capable of detecting *L. monocytogenes* at the point of sampling. In this context, AuNP-based colorimetric biosensors offer a powerful combination of visual simplicity, molecular specificity, and operational portability.

The present study aimed to develop and validate a gold nanoparticle (AuNP)-based colorimetric biosensor using oligonucleotide-functionalized probes targeting the *hly* gene of *L. monocytogenes*. The assay was designed to provide rapid (≤30 min) visual detection through salt-induced aggregation monitored via LSPR at 520–530 nm. Analytical sensitivity and specificity were evaluated using reference strains and compared with conventional methods including VITEK-2, MALDI-TOF, and PCR. Furthermore, the biosensor's applicability was tested on dairy products, including raw milk, yogurt, Kareish cheese, and soft ice cream collected from retail outlets in Beni-Suef, Egypt.

By integrating nanotechnology with molecular diagnostics, this work proposes an alternative, rapid, and sensitive platform for *L. monocytogenes* detection that merges the simplicity of lateral flow assays with the precision of nucleic acid hybridization. The developed AuNP-based system has the potential to enhance on-site food safety monitoring and contribute to early intervention strategies for preventing listeriosis outbreaks.

Materials and methods

Samples collection

A total of 200 samples, including raw milk, small-scale yogurt, Kareish cheeses, and soft ice cream (50 samples each) were collected aseptically from retail outlets in Beni-Suef Governorate, Egypt, using sterile plastic containers. The collected samples were transported on ice to the laboratory and immediately analyzed to detect *L. monocytogenes* upon arrival.

Isolation of Listeria monocytogenes

L monocytogenes was isolated from the collected samples as previously described (Roberts and Green wood, 2003). Twenty-five ml/g of each sample was homogenized with 225 ml of buffered *Listeria* enrichment broth (BLEB) base (Himedia, India) supplemented with selective agent (Himedia, India), and the samples were incubated at 30°C for 48 h. A loopful of the BLEB grown cultures was streaked on *Listeria* Oxford agar (Himedia, India), supplemented with *Listeria* selective supplement, then incubated at 35±2°C for 24-48 h. The characteristic green to brown colonies with black haloes were picked and streaked onto Tryptic soy agar supplemented with 0.6% (w/v) yeast extract (Oxoid, UK) for identification. The collected isolates were investigated for morphological and biochemical characteristics, including Gram staining, catalase and oxidase production, carbohydrate utilization, nitrate reduction, β-haemolysis, motility at 25°C, and CAMP test.

Identification of L. monocytogenes using PCR

PCR was performed to identify the presumptive *L. monocytogenes* isolates via the amplification of the *hly* gene by using 5′-CCTAAGACG-CCAATCGAA-3′ and 5′-AAGCGCTTGCAACTGCTC-3′ primers (Chen *et al*., 2017). The PCR reaction was carried out in a total volume of 50 µL by mixing 5 µL 10X Dream Taq buffer, 50 ng genomic DNA template, 0.4 µM of each primer, 0.2 mM of each dNTP, and one Unit Dream Taq DNA polymerase (Thermo Scientific, USA). The amplification program contained an initial denaturation step at 95°C for 4 min, followed by 30 cycles of denaturation at 95°C for 30 s, annealing at 55°C for 30 s, extension at 72°C for 60 s, and a final extension at 72°C for 8 min in a ProFlex thermocycler. Subsequently, the amplicons were subjected to 1.5% agarose gel electrophoresis, and gels were analysed by a chemiPRO gel documentation system (Clever, UK).

Automated biochemical identification of L. monocytogenes using VITEK 2

The presumptive *L. monocytogenes* isolates were identified by the VITEK-2 compact system (BioMerieux, France). Briefly, each isolate was aseptically resuspended in 3.0 ml of sterile saline and density was adjusted to a McFarland 0.50–0.63 using a DensiChek (BioMerieux, France). Subsequently, the identification cards and polystyrene test tubes with the suspensions were placed in the VITEK-2 Compact cassette and the identification was conducted according to the procedure indicated by the manufacturer.

Identification of L. monocytogenes using MALDI-TOF/MS

The identification was also confirmed using Matrix-Assisted Laser Desorption-Time of Flight (MALDI-TOF). Briefly, a single colony from a fresh overnight culture of presumptive positive isolates was smeared as a thin film directly onto a MALDI target plate using a sterile stick and allowed to dry. Then, 1 µL of alpha-cyano-4-hydroxycinnamic acid matrix solution was added to the spots and allowed to dry. Thereafter, the slides were introduced into the LT2 Plus MALDI-TOF/MS (SAI, UK), and the obtained mass spectra were analyzed by the BactoSCREEN-ID V2.4 software (SAI, UK).

Identification of L. monocytogenes by optical biosensing using oligonucleotide-gold nanoparticles

Synthesis and characterization of gold nanoparticles

AuNPs were synthesized using the citrate reduction method with some modifications (Lin *et al*., 2008). Briefly, 10 ml of 1% trisodium citrate was quickly added to 100 ml of boiling HAuCl4 solution (1 mM) with vigorous stirring. The mixture was boiled continuously and stirred for 15 min, until the color changed from faint yellow to a bright ruby-red. Subsequently, the produced nanoparticles were collected by centrifugation at 50,000 ×g for 20 min and washed twice with ultrapure water to remove any un-reactants. Finally, AuNPs were resuspended in ultrapure water and stored at 4°C. Afterwards, UV-Vis spectroscopy was conducted in the 300–700 nm range using an Epoch 2 UV–Vis spectrophotometer (BioTek, USA) to identify the characteristic surface plasmon resonance peak, confirming the formation of AuNPs. The morphology and size of AuNPs were investigated by high-resolution transmission electron microscopy (HRTEM) using a JEM-2100 transmission electron microscope (JEOL, Japan) operating at 200 kV. Furthermore, the size distribution and

zeta potential of the prepared AuNPs were determined using a Nano-ZS particle size analyser (Malvern Instruments Ltd., UK). The X-ray diffraction (XRD) pattern was analysed on a D8 Discover X-ray diffractometer (Bruker, Germany), and the 2θ values were measured in a range from 20 to 90°. The elemental analysis was performed using a Quattro S instrument (Thermo Scientific, USA) equipped with energy-dispersive X-ray spectroscopy (EDX).

Designing oligonucleotide primers and probes

In this work, two sets of asymmetric PCR (asPCR) primers and thiol-modified oligonucleotide probes were designed to target the Listeriolysin O gene (*hly*) of *L. monocytogenes* based on the *hly* gene sequence of *L. monocytogenes* strain ATCC 13932 (GenBank accession no. JN703912.1) and the complete genome sequence of *L. monocytogenes* strains ATCC 19115 and ATCC 19117 (GenBank accession no. CP177353.1 and CP013288.1, respectively). Accordingly, the asPCR primers Lm-192F 5′-GTGCCGCCAAGAAAAGGTTA-3′ and Lm-192R 5′ ACGTTTGACAG-GAAGAACATCG-3′ and thiol-modified oligonucleotides with sequences [P1-Lm: 5′-SH-(CH2)6 GATTTTCTACTAATTCCGAATTCGCTTTCA-3′) and (P2-Lm: 5′GTTAGGCTCGAAATTGCATTCACAACTTGG-(CH2)6-SH-3′], respectively, were designed and then synthesized by Eurogentec ltd (Kaneka Eurogentec S.A, Liege Science Park, Seraing, Belgium).

Synthesis of AuNPs-oligonucleotide probes

To develop an AuNPs-based optical biosensing system, each of the two thiol-modified oligonucleotide probes was conjugated separately onto the surface of AuNPs following the method described by Quintela *et al*. (2019). In brief, 20 µL of each thiol-modified oligonucleotide probe (20 µM) was added to 980 µL of AuNPs solution and then subjected to increasing salt concentration (0.05–1.0 M NaCl in 10 mM Na_2HPO_4, pH 7.4) for 24 h in a water bath at 37°C. Subsequently, the mixtures were centrifuged at 20,000 ×g for 30 min to remove the unbound probes, while the remaining oily-like AuNPs were resuspended in salt buffer solution (NaCl in 10 mM Na_2HPO_4, pH 7.4). Finally, the prepared AuNPs-oligonucleotide probes were kept in dark conditions at 4°C until further use.

Citrate-reduced AuNPs were functionalized with single-stranded thiolated oligonucleotides via thiol–gold (Au–S) covalent bonding. Briefly, oligonucleotides carrying a 5′- or 3′-terminal thiol group [HS–$(CH_2)_6$] were incubated with the colloidal AuNPs, and gradual salt aging was performed by successive additions of NaCl until a final concentration of 1 M in 10 mM phosphate buffer (pH 7.4) was reached. This procedure enhances DNA loading on AuNPs and provides stable salt-resistant conjugates suitable for downstream biosensing applications.

AuNPs optical biosensing assay

The developed AuNPs optical biosensing assay was evaluated on pure cultures of *L. monocytogenes* strain ATCC 13932 and *L. monocytogenes* ATCC 19117. The genomic DNA was extracted from each strain using a PureLink DNA Purification Kit (Thermo Scientific, USA), and the asPCR was conducted to produce a single-stranded PCR product of the *hly* gene using Lm-192F and Lm-192R primers and 50 ng of genomic DNA of *L. monocytogenes*. The amplification was performed in a ProFlex thermocycler (Applied Biosystems, USA) with an initial denaturation step at 95°C for 4 min, followed by 30 cycles of denaturation at 95°C for 30 s, annealing at 58°C for 30 s, extension at 72°C for 30 s, and a final extension at 72°C for 8 min. Blank reactions were performed in the same conditions with the addition of nuclease-free water instead of DNA templates. Subsequently, the DNA sandwich hybridization was performed by mixing the asPCR products (50 µL) or blank with 50 µL of each AuNPs-oligonucleotide probe, and the mixture was incubated for 30 min at 55°C. Then, a salt solution (NaCl in 10 mM Na_2HPO_4, pH 7.4) was added to a final concentration of 2 M NaCl, and the color changes in various reaction mixtures were observed within 5 min (Quintela *et al*., 2019). Also, the absorbance of the reaction mixtures was measured in the range of 300 to 700 nm using an Epoch 2 UV–Vis spectrophotometer.

Evaluation of specificity

To evaluate the specificity of the developed biosensing assay toward *L. monocytogenes*, the assay was investigated against some common foodborne bacterial pathogens. The investigated strains were *L. monocytogenes* ATCC 19117, *L. monocytogenes* ATCC 13932, *L. ivanovii* ATCC 19119, *Bacillus cereus* ATCC 14579, *Staphylococcus aureus* subsp. *aureus* ATCC 6538, *Escherichia coli* ATCC 8739, *Salmonella enterica* subsp. *enterica* ATCC 14028, and *Pseudomonas aeruginosa* ATCC 9027. The genomic DNA was extracted from each bacterial strain and used as a template for asPCR, and the AuNPs optical biosensing assay was performed as described above.

Evaluation of sensitivity

The sensitivity of the developed biosensing assay was evaluated at various levels of *L. monocytogenes* genomic DNA. Briefly, asPCR was performed using genomic DNA templates ranging from 1 pg to 1 ng/µL, then the AuNPs optical biosensing assay was performed as described above.

Application of AuNPs-oligonucleotide probe optical biosensing for the detection of L. monocytogenes

To detect the presence of *L. monocytogenes* in raw milk and dairy products using an AuNPs-oligonucleotide probe optical biosensing assay, genomic DNA was extracted from post-enriched samples and used as a template for asPCR. Subsequently, DNA sandwich hybridization was performed by mixing the asPCR products and AuNPs-oligonucleotide probes, followed by the addition of NaCl solution (final concentration of 2 M), and the color change was observed as described above.

Results

Isolation and identification of L. monocytogenes using biochemical and PCR assays

Nine presumptive positive *Listeria monocytogenes* were recovered from the examined samples using *Listeria* Oxford selective media. Based on the cultural, morphological, and biochemical properties of the isolated strains, they were found to be catalase, methyl red, beta-hemolytic, CAMP-positive, and Gram-positive non-sporulating rods. Although the above-mentioned *Listeria* Oxford media contains selective agents to inhibit the growth of most microorganisms other than *L. monocytogenes*, some other bacteria have the ability to grow and utilize esculin (i.e., Enterococcus and Bacillus), resulting in a similar appearance , indicating the requirement for further tests to definitely identify the isolated *Listeria* colonies. Therefore, these isolates were further characterized using PCR, VITEK-2, MALDI-TOF, and AuNPs-Oligonucleotide probes for identification. Out of the isolated strains, 6 (66.7%) isolates were confirmed by PCR as *L. monocytogenes* (Table 1). Based on PCR results, the incidence of *L. monocytogenes* in raw milk, small-scale yogurt, Kareish cheese, and soft ice cream was 4.0, 0.0, 8.0, and 0.0%, respectively, as shown in Table 1.

VITEK-2 system identification and characterization of L. monocytogenes isolates.

The isolates were further characterized using the VITEK-2 system for species identification. Among nine isolates, 6 (66.7%) were confirmed as *L. monocytogenes* and 3 (33.3 %) were not confirmed as (one isolate was

Table 1 Prevalence of *L. monocytogenes* in the examined dairy products samples.

Product	No. of the examined samples	Presumptive *L. monocytogenes* samples	Confirmed *L. monocytogenes* samples	
			No.	Percentage
Raw milk	50	3	2	4.00%
Small scale yogurt	50	0	0	0.00%
Kareish cheese	50	6	4	8.00%
Soft ice cream	50	0	0	0.00%
Total	200	9	6	3.00%

confirmed as *L. innocua* (11.1%) and 2 isolates their confidence were with low discrimination). All six *Listeria* isolates identified as *L. monocytogenes* by PCR were also identified as positive, using the VITEK-2 system (Table 2).

MALDI-TOF/MS identification and characterization of L. monocytogenes isolates

Among nine isolates, 6 (66.7%) were confirmed as *L. monocytogenes* using MALDI-TOF/MS. On the other hand, three (33.3%) presumptive isolates were identified as *Bacillus cereus* (11.1%), *Aneurinibacillus aneurinilyticus* (11.1%), and *L. innocua* (11.1%) using the MALDI-TOF assay (Table 3).

Identification of L. monocytogenes isolates using AuNPs-Oligonucleotide probs

Characterization of AuNPs

Transmission electron microscopy (TEM) analysis revealed that the synthesized AuNPs were predominantly spherical in shape and uniformly dispersed without signs of aggregation (Fig. 1A). Size analysis of 50 particles indicated that the diameters ranged from 8 to 17 nm, with an average size of 11.7±2.2 nm and a median of 11.5 nm (Fig. 1B). These findings were further supported by dynamic light scattering (DLS) measurements, which showed a narrow size distribution with an average particle size of 20 nm (Fig. 1C). The electrical double layer's zeta potential, or dispersion surface charge, is a crucial characteristic that indicates the stability of the colloidal particles in the solution. The AuNPs are stable colloids in the solution, as indicated by the average value of the Zeta potential of 29.4 mV (Fig. 1D). The repulsive force between the colloidal AuNPs is represented by the negative value of the Zeta potential. Collectively, these findings confirm the successful synthesis of stable, monodisperse AuNPs with nanoscale dimensions.

Colorimetric detection of *L. monocytogenes* by using AuNP-probe conjugates as indicators

The amplified *L. monocytogenes* ATCC 19117 strains were tested along with *L. monocytogenes* ATCC 13932 and nuclease-free water as the blank. It was simultaneously observed by the naked eye that the reaction mixture wells of different *L. monocytogenes* strains remained red in color, while the wells containing blank turned purplish-blue when the salt solution (final concentration of 2 M) was added (Fig. 2A, B). After adding salt solution, the oligonucleotide/AuNPs probes maintained their original red hue, indicating a successful hybridization with their corresponding area. This is explained by the way DNA sandwich hybridization created a network and complexes that kept AuNPs stable even at higher salt concentrations. Out of nine presumptive positive *L. monocytogenes* isolates recovered from 200 examined samples, six were confirmed positive using AuNPs-Oligonucleotide probes, while three were determined to be false positives. A fingerprint peak in the absorbance spectra of AuNPs is visible between 500 and 600 nm (520- 530), which is indicative of the particles' localized surface plasmon resonance (LSPR) (Fig. 2C, D).

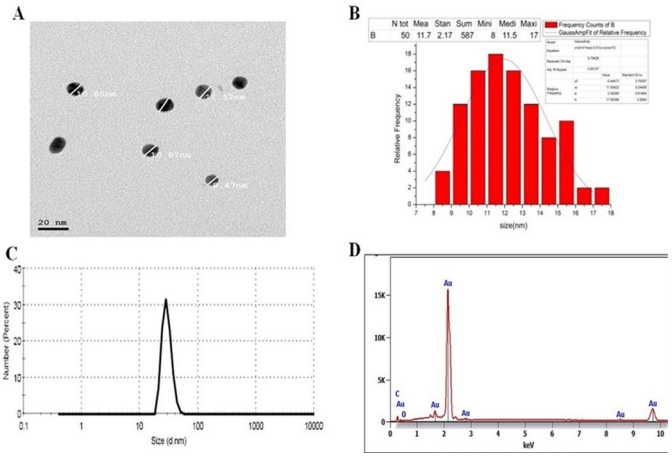

Fig. 1. Characterization of the synthesized AuNPs. (A). TEM images showing the size and morphology of the synthesized AuNPs with the measured diameter. (B). Histogram displays the size distribution of AuNPs, mean size (11.7 nm), standard deviation (2.17 nm), minimum and maximum sizes observed, and the total number of data points (50) are among the statistical characteristics shown in the table in the upper right. (C). Dynamic light scattering (DSL) analysis confirming the size distribution AuNPs, with a narrow peak indicating monodisperse nanoparticles. (D). Energy Dispersive X-ray (EDX) spectrum confirming the presence of synthesized AuNPs with a characteristic peak.

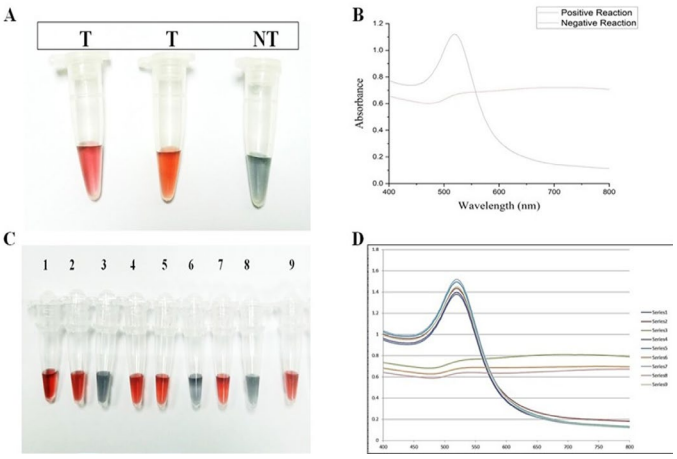

Fig. 2. (A). AuNPs optical biosensing of *L. monocytogenes* showing two reactions, mixture after adding salt solution final reaction. NT sample changed from red to bluish-purple color while no color change was observed in T reaction mixture. NT: non target nuclease-free water as blank. T: targeted *L. monocytogenes* ATCC 19117 and *L. monocytogenes* ATCC 13932. (B). UV-Vis absorption spectra for the colorimetric detection of *L. monocytogenes* using AuNP- oligonucleotide probes, showing positive and negative reactions. (C). Colorimetric detection of *L. monocytogenes* by AuNPs-oligonucleotide probes. 1, 2, 4, 5, 7, and 9 red colored tubes indicate positive samples, while 3, 6, and 8 blue colored tubes indicate false positive samples. (D). UV-Vis absorption spectra for the colorimetric detection of *L. monocytogenes* using AuNP- Oligonucleotide Probes, showing subphase plasmon resonance (SPR) peak at ~520–530 nm and spectral variations indicating different hybridization conditions.

AuNPs optical biosensing assay

The *L. monocytogenes hly*A gene was amplified using PCR. To verify the specificity of the primers, the same procedure was used with strains of *L. ivanovii* ATCC 19119, *Bacillus cereus* ATCC 14579, *Staphylococcus aureus* subsp. aureus ATCC 6538, *E. coli* ATCC 8739, *Salmonella enterica* subsp. Enterica ATCC 14028, and *Pseudomonas aeruginosa* ATCC 9027. The *hly*AF and *hly*AR primers were specific for the *hly*A gene of *L. monocytogenes*, according to an agarose gel electrophoresis. These primers primarily guaranteed the specificity of the AuNP-probe conjugates used to identify the *hly*A gene and *L. monocytogenes* genomic DNA (Fig. 3).

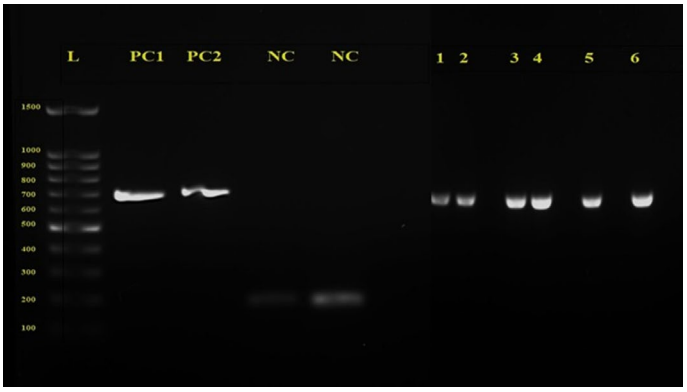

Fig. 3. PCR amplification of *L. monocytogenes*. Target Gene at 702 bp (Lane L: 100 bp DNA ladder; Lane PC1: Positive Control (*L. monocytogenes* ATCC 19117), PC2: Positive Control (*L. monocytogenes* ATCC 13932); NC: Negative Control; Lanes 1-6, amplified *L. monocytogenes* positive samples).

Specificity and sensitivity

The specificity of the colorimetric assay based on AuNP-probe conjugates was further confirmed when the genomic DNA used as a control in the colorimetric experiment resulted in a colorless solution (Fig. 4A).

As seen in Fig. 4B, C, the AuNPs optical biosensing's sensitivity was tested on a range of *Listeria* spp. DNA concentrations. At 1 pg/µL, 2 pg/µL, 5 pg/µL, 10 pg/µL, 50 pg/µL, 100 pg/µL, 200 pg/µL, 500 pg/µL, and 1 ng of *L. monocytogenes* ATCC 19117 demonstrated positive results at 10 pg/µL, but negative results for blank (nuclease-free water). There was no discernible color shift, yet both the blank and non-target turned purple blue on the remaining target samples. The absorbance peak of AuNPs and AuNP probe conjugates was 610 and 525 nm for several *Listeria* spp. strain's reaction mixes (10 pg/µL) following the addition of salt. The red shift was related to the fact that the surface of AuNPs has been attached with the probe. These findings demonstrate that *Listeria* spp. strains have been successfully and concurrently identified by the AuNPs optical biosensor via *hly* at 10 pg/µL. According to statistically valid results and color change differentiation, the AuNPs optical biosensor has a DL of less than 10 pg/µL and 100% specificity. A positive detection of the target DNA is indicated by the red tubes, which validate hybridization with complimentary sequences. The tubes that have gone gray indicate that AuNPs were not detected or aggregated, most likely because the target DNA was not present. The distinct hue shift observed between positive and negative samples demonstrates the effectiveness of AuNPs as a visual signal for detecting specific DNA sequences. Additionally, these findings were consistent with the TEM and gel electrophoresis results.

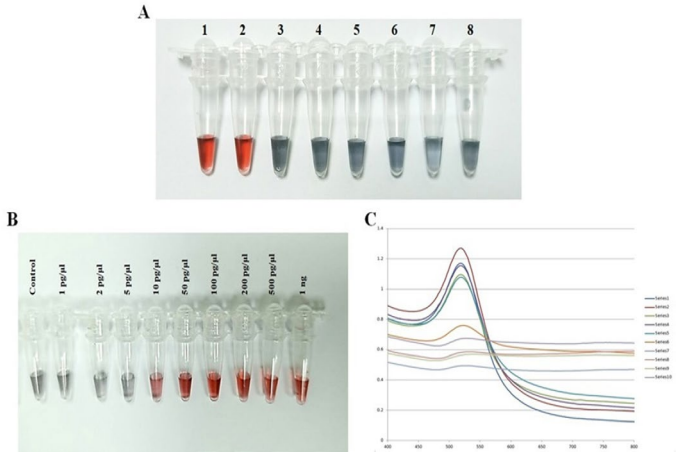

Fig. 4. (A). Specificity of DNA probe assay against *L. monocytogenes*. 1. positive control of *L. monocytogenes* ATCC 19117, 2. *L. monocytogenes* ATCC 13932, 3. *L. ivanovii* ATCC 19119, 4. *Bacillus cereus* ATCC 14579, 5. *Staphylococcus aureus* subsp. aureus ATCC 6538, 6. *E. coli* ATCC 8739, 7. *Salmonella enterica* subsp. Enterica ATCC 14028, and 8. *Pseudomonas aeruginosa* ATCC 9027. (B). Colorimetric sensitivity test using *hly*A gene. At DNA concentrations of negative control, 1 pg/µL, 2 pg/µL, 5 pg/µL, 10 pg/µL, 50 pg/µL, 100 pg/µL, 200 pg/µL, 500 pg/µL, and 1 ng with a detection limit of 10 pg/µL. (C). Vis spectrum detection *hly*A gene. 1-6 AuNP-probe with complementary DNA target showing surface plasmon resonance (SPR) shifts indicative of DNA hybridization.

Table 2 Identification of presumptive *L. monocytogenes* using VITEK-2 assay.

Strain	No. of Samples	Percentages
L. monocytogenes	6	66.70%
L. innocua	1	11.10%
low discrimination strains	2	22.20%

Table 3 Identification of presumptive *L. monocytogenes* using MALDI-TOF/MS.

Strain	No. of Samples	Percentages
L. monocytogenes	6	66.70%
L. innocua	1	11.10%
Bacillus cereus	1	11.10%
Aneurinibacillus aneurinilyticus	1	11.10%

Discussion

The overall contamination rate of 3.0% observed here is within the lower range of global and regional reports. Abbas and Jaber (2012) found 11% *L. monocytogenes* contamination in raw cow milk, while Moosavy *et al.* (2014) reported 50% among 18 milk samples from Iran. Similarly, prevalence values of 8.8%, 8%, 25%, and 6% were reported by Abd El-Tawab *et al.* (2015); Tahoun *et al.* (2017); Biswas *et al.* (2018) and James *et al.* (2018), respectively. In contrast, Fadel (2016) and Borena *et al.* (2022) reported much lower rates (1.1–3.3%) in milk samples analyzed by PCR and MALDI-TOF. The current prevalence of 8.0% in Kareish cheese is slightly higher than that reported by Kahraman *et al.* (2010); Fadel (2016), and Abd El-Tawab *et al.* (2015), but is comparable to the 6.7% reported by Ewida *et al.* (2022) and Kayode and Okoh (2022) for soft cheese. The absence of *L. monocytogenes* in yogurt and soft ice cream aligns with Ewida *et al.* (2022) and Fadel (2016), but lower than the prevalence reported by Abd El-Tawab *et al.* (2015) and Biswas *et al.* (2018), who observed rates ranging from 6 to 12% in ice cream. Such discrepancies likely reflect differences in sampling locations, hygiene standards, and seasonal variations.

Out of 200 examined dairy samples, only six (3.0%) were confirmed positive for *Listeria monocytogenes* using advanced identification methods, including PCR, VITEK-2, MALDI-TOF/MS, and AuNPs-based optical

probes. Although nine presumptive isolates were initially recovered on Oxford agar, confirmatory identification reduced this number, reflecting the limitations of selective media. This outcome agrees with previous reports indicating that Oxford medium, while efficient for preliminary screening, can yield false positive results due to the growth of other esculin-hydrolyzing organisms such as Bacillus and Enterococcus spp. (Osek *et al*., 2022). Morphological similarities between *Listeria* and species such as *Bacillus cereus* or *Aneurinibacillus aneurinilyticus* may also contribute to misidentification, underscoring the importance of proteomic and molecular confirmation for diagnostic accuracy.

The confirmed prevalence of *L. monocytogenes* varied among product types, with the highest rate observed in Kareish cheese (8.0%), followed by raw milk (4.0%), whereas soft ice cream and small-scale yogurt showed no verified presence. These differences likely reflect variations in hygiene practices, processing control, and the use of unpasteurized milk in artisanal production. Traditional Kareish cheese is commonly produced under non-standardized conditions, which can facilitate post-processing contamination. Our findings are consistent with prior studies from Egypt and neighboring regions, which reported prevalence rates ranging from 4–10% in raw milk (El-Demerdash and Raslan 2019; Saleh *et al*., 2021) and 5–26% in local dairy products (Abd El-Tawab *et al*., 2015; Tahoun *et al*., 2017; Abdeen *et al*., 2021). Collectively, these results confirm that artisanal and small-scale dairy products pose higher microbiological risks than industrially processed ones.

The VITEK-2 automated biochemical system correctly identified 66.7% of presumptive isolates as *L. monocytogenes*, showing high concordance with PCR targeting the *hly*A gene. MALDI-TOF/MS provided an equally reliable classification, successfully distinguishing *L. monocytogenes* from non-target organisms. These results align with those reported by Guo *et al*. (2014), who demonstrated that MALDI-TOF can accurately identify *Listeria* species when an updated spectral library is used. However, three isolates initially classified as *L. monocytogenes* were later re-identified as *Bacillus cereus*, *Aneurinibacillus aneurinilyticus*, and *L. innocua*, respectively. This reinforces the need for complementary proteomic or molecular validation, especially when using biochemical or culture-based systems that rely on phenotypic profiles susceptible to overlap.

PCR and real-time PCR assays remain the gold standard for *L. monocytogenes* detection, capable of identifying as few as 8–10 CFU based on amplification of the *hly* gene (Gianfranceschi *et al*., 2014). Nevertheless, these methods require sophisticated instruments, trained personnel, and post-amplification handling, making them less practical for field applications or resource-limited laboratories. To overcome these constraints, the present study developed and validated an alternative AuNP-based optical biosensor for rapid, equipment-free detection (Mocan *et al*., 2017).

The developed colorimetric biosensor utilized thiolated single-stranded DNA oligonucleotides conjugated to citrate-reduced gold nanoparticles (AuNPs) to detect the *hly*A gene of *L. monocytogenes*. The detection mechanism is based on localized surface plasmon resonance (LSPR), a phenomenon in which light induces collective oscillation of conduction electrons on AuNP surfaces, producing a visible red color that was utilized in the optical biosensor. Upon hybridization with complementary target DNA, the solution retains its red hue; in contrast, non-target or blank samples display a purple-blue shift after salt addition, indicating nanoparticle aggregation due to unsuccessful hybridization (Park and You 2023). This color change provides an immediate, visually interpretable result without the need for specialized instruments, establishing the foundation for a sensitive, reliable, and user-friendly detection platform.

The biosensor's physical properties were verified using TEM and UV–Vis spectroscopy. The synthesized AuNPs exhibited a uniform spherical morphology with an average diameter of ~11.7 nm, a sharp LSPR absorption peak at 520–530 nm, and excellent stability confirmed by a zeta potential of −29.4 mV. These parameters are consistent with optimal nanoparticle characteristics for biosensing, where high monodispersity and strong negative surface charge prevent aggregation (Karnwal *et al*., 2024; Tirkey and Babu 2024). The observed narrow LSPR peak further confirms colloidal stability and homogeneity, both critical for reproducible colorimetric response (Dheyab *et al*., 2022; Jia *et al*., 2022).

Following hybridization, only DNA from *L. monocytogenes* ATCC strains produced a red color, demonstrating excellent specificity toward the *hly*A gene. Other tested bacteria, including *Salmonella enterica*, *Staphylococcus aureus*, and *Escherichia coli*, elicited no color change (Laximan *et al*., 2016). Sensitivity testing revealed a detection limit below 10 pg/µL, which is remarkable for a visual assay and comparable to advanced molecular systems. UV-Vis spectral analysis confirmed a red shift in LSPR associated with hybridization events, supporting visual observations. The assay achieved 100% specificity and outstanding sensitivity, making it ideal for on-site applications, routine diagnostics, and potential quarantine surveillance. Comparable LAMP-AuNP/DNA probe systems have shown similar specificity to PCR-based techniques, with no cross-reactivity to closely related bacterial species (Wachiralurpan *et al*., 2018).

The average AuNP size (~11.7 nm) falls within the optimal range (< 30 nm) for biosensing applications due to enhanced surface-area-to-volume ratio, which facilitates efficient probe immobilization (Bharadwaj *et al*., 2021). The zeta potential value (−29.4 mV) suggests strong electrostatic repulsion preventing aggregation, confirming colloidal stability (Karnwal *et al*., 2024). The negative surface charge is attributed to citrate capping, known for stabilizing AuNPs through electrostatic interactions (Tirkey and Babu, 2024).

The characteristic LSPR peak at 520–530 nm represents the optical fingerprint of spherical AuNPs (Xiao *et al*., 2023). Peak broadening or redshift typically signals aggregation or irregular morphologies, whereas sharp, symmetric peaks indicate monodispersity (Jia *et al*., 2022). In this study, the narrow LSPR bandwidth implies uniform particle size and excellent dispersion. Such stability is vital because salt-induced aggregation or biomolecular fouling often compromises biosensor reproducibility (Badir *et al*., 2025). Hence, the synthesized AuNPs exhibit ideal physicochemical traits for reliable biosensing.

The current results corroborate growing evidence that nanomaterial-based colorimetric biosensors can provide high-fidelity detection of foodborne pathogens. Advantages of the developed AuNP assay include fast visible results, label-free detection, high selectivity, and minimal instrumentation. These findings align with recent reports describing AuNP biosensors as efficient alternatives for food safety diagnostics (Du *et al*., 2018; Soni *et al*., 2018; Inês and Cosme 2025). Compared to ELISA or qPCR, AuNP-based assays are faster, cost-effective, and operationally simpler, while maintaining comparable analytical accuracy.

Conclusion

This study successfully developed a thiolated single-stranded oligonucleotide-functionalized gold nanoparticle (AuNP)-based colorimetric biosensor for the rapid and specific detection of *Listeria monocytogenes* in dairy products. The synthesized AuNPs (≈11.7–20 nm) exhibited excellent colloidal stability and a distinct LSPR peak at 520–530 nm. The biosensor, targeting the *hly*A gene, achieved a detection limit of 10 pg/µL and 100% specificity, effectively differentiating true positives from false-positive isolates. The confirmed prevalence of *L. monocytogenes* was 4.0% in raw milk and 8.0% in Kareish cheese, while yogurt and soft ice cream were negative. These findings highlight the biosensor's potential as a rapid, sensitive, and cost-effective diagnostic tool for *L. monocytogenes*, offering a promising alternative to conventional molecular and culture-based assays. Its simplicity and visual readout make it suitable for routine food safety surveillance and on-site pathogen monitoring.

Conflict of interest

The authors have no conflict of interest to declare.

References

Abbas, B.A., Jaber, G.M., 2012. Occurrence of *Listeria monocytogenes* in raw milk of ruminants in Basrah province. Iraqi Journal of Veterinary Sciences 26, 47–51. https://doi.org/10.33899/ijvs.2012.46959

Abd El-Tawab, A.A., Maarouf, A.A.A., Mahy, Z.A.M., 2015. Bacteriological and molecular studies of *Listeria* species in milk and milk products at El-Kaliobia Governorate. Benha Veterinary Medical Journal 29, 170–180. https://doi.org/10.21608/bvmj.2015.31698

Abdeen, E.E., Mousa, W.S., Harb, O.H. Fath-Elbab, G.A., Nooruzzaman, M., Gaber, A., Alsanie, W.F., Abdeen, A., 2021. Prevalence, antibiogram and genetic characterization of *Listeria monocytogenes* from food products in Egypt. Foods 10, 1381. https://doi.org/10.3390/foods10061381

Angelo, K.M., Conrad, A.R., Saupe, A., Dragoo, H., West, N., Sorenson, A., Barnes, A., Doyle, M., Beal, J., Jackson, K.A., Stroika, S., Tarr, C., Kucerova, Z., Lance, S., Gould, L.H., Wise, M., Jackson, B.R., 2017. Multistate outbreak of *Listeria monocytogenes* infections linked to whole apples used in commercially produced, prepackaged caramel apples: United States, 2014–2015. Epidemiology and Infection 145, 848–856. https://doi.org/10.1017/S0950268816003083

Araújo, T.M.C., Pereira, R.C.L., Freitag, I., Rusak, L., Botelho, L., Hofer, E., Hofer, C., Vallim, D., 2020. Evaluation of MALDI-TOF MS as a tool for detection of *Listeria* spp. directly from selective enrichment broth from food and stool samples. Journal of Microbiological Methods 173, 105936. https://doi.org/10.1016/j.mimet.2020.105936

Badir, A., Refki, S., Sekkat, Z., 2025. Utilizing gold nanoparticles in plasmonic photothermal therapy for cancer treatment. Heliyon 11, e42738. https://doi.org/10.1016/j.heliyon.2025.e42738

Bharadwaj, K.K., Rabha, B., Pati, S., Sarkar, T., Choudhury, B.K., Barman, A., Bhattacharjya, D., Srivastava, A., Baishya, D., Edinur, H.A., Abdul Kari, Z., Mohd Noor, N.H., 2021. Green synthesis of gold nanoparticles using plant extracts as beneficial prospect for cancer theranostics. Molecules 26, 6389. https://doi.org/10.3390/molecules26216389

Biswas, P., Deka, D., Motina, E., Dutta, T.K., Singh, N.S., 2018. Studies on detection and antibiotic sensitivity and resistance pattern of *Listeria monocytogenes* isolated from cattle, raw cow milk and milk products from Tripura, India. International Journal of Chemical Studies 6, 190–196

Borena, B.M., Dilgasa, L., Gebremedhin, E.Z., Sarba, E.J., Marami, L.M., Kelbesa, K.A., Tadese, N.D., 2022. *Listeria* species occurrence and associated risk factors and antibiogram of *Listeria monocytogenes* in milk and milk products in Ambo, Holeta, and Bako towns, Oromia Regional State, Ethiopia. Veterinary Medicine International 2022, 1–11. https://doi.org/10.1155/2022/5643478

Buchanan, R.L., Gorris, L.G., Hayman, M.M., Jackson, T.C., Whiting, R.C., 2017. A review of *Listeria monocytogenes*: an update on outbreaks, virulence, dose-response, ecology, and risk assessments. Food Control 75, 1–13. https://doi.org/10.1016/j.foodcont.2016.12.016

Chen, J.-Q., Healey, S., Regan, P., Laksanalamai, P., Hu, Z., 2017. PCR-based methodologies for detection and characterization of *Listeria monocytogenes* and *Listeria* ivanovii in foods and environmental sources. Food Science and Human Wellness 6(2), 39–59. https://doi.org/10.1016/j.fshw.2017.03.001

Dapgh, A., Salem, R.L., 2022. Molecular detection of *Listeria monocytogenes* in milk and some milk products. International Journal of Veterinary Science 11, 514–519. https://doi.org/10.47278/journal.ijvs/2021.128

De Lappe, N., Lee, C., O'Connor, J., Cormican, M., 2014. Misidentification of *Listeria monocytogenes* by the VITEK 2 system. Journal of Clinical Microbiology 52, 3494–3495. https://doi.org/10.1128/JCM.01725-14

de Noordhout, C.M., Devleesschauwer, B., Angulo, F.J., Verbeke, G., Haagsma, J., Kirk, M., Havelaar, A.H., Speybroeck, N., 2014. The global burden of listeriosis: a systematic review and meta-analysis. The Lancet Infectious Diseases 14, 1073–1082. https://doi.org/10.1016/S1473-3099(14)70870-9

Dheyab, M.A., Aziz, A.A., Moradi Moradi, K.P., Jameel, M.S., Oladzadabbasabadi, N., Mohammed, S.A., Abdullah, R.S., Mehrdel, B., 2022. Monodisperse gold nanoparticles: a review on synthesis and their application in modern medicine. International Journal of Molecular Sciences 23, 7400. https://doi.org/10.3390/ijms23137400

Du, J., Singh, H., Dong, W., Bai, Y., Yi, T.-H., 2018. Colorimetric detection of *Listeria monocytogenes* using one-pot biosynthesized flower-shaped gold nanoparticles. Sensors and Actuators B: Chemical 265, 285–292. https://doi.org/10.1016/j.snb.2018.03.067

EFSA and ECDC., 2021. The European Union One Health 2020 zoonoses report. EFSA Journal 19, e06971. https://doi.org/10.2903/j.efsa.2021.6971

El-Demerdash, A.S., Raslan, M.T., 2019. Molecular characterization of *Listeria monocytogenes* isolated from different animal-origin food items from urban and rural areas. Advances in Animal and Veterinary Sciences 7, 51–56. https://doi.org/10.17582/journal.aavs/2019/7.s2.51.56

Ewida, R.M., Hasan, W.S., Elfaruk, M.S., Alayouni, R.R., Hammam, A.R.A., Kamel, D.G., 2022. Occurrence of *Listeria* spp. in soft cheese and ice cream: effect of probiotic *Bifidobacterium* spp. on survival of *Listeria monocytogenes* in soft cheese. Foods 11, 3443. https://doi.org/10.3390/foods11213443

Ferreira, V., Wiedmann, M., Teixeira, P., Stasiewicz, M.J., 2014. *Listeria monocytogenes* persistence in food-associated environments: epidemiology, strain characteristics, and implications for public health. Journal of Food Protection 77, 150–170. https://doi.org/10.4315/0362-028X.JFP-13-150

Fadel, H., 2016. Detection of *Listeria monocytogenes* in raw milk and ready-to-eat dairy products with evaluating the antimicrobial effect of cold-pressed Nigella sativa oil. Assiut Veterinary Medical Journal 62, 13–18. https://doi.org/10.21608/avmj.2016.169960

Gianfranceschi, M.V., Rodriguez-Lazaro, D., Hernandez, M., González-García, P., Comin, D., Gattuso, A., Delibato, E., Sonnessa, M., Pasquali, F., Prencipe, V., Sreter-Lancz, Z., Saiz-Abajo, M.-J., Pérez-De-Juan, J., Butrón, J., Kozačinski, L., Horvatek Tomic, D., Zdolec, N., Johannessen, G.S., Jakočiūnė, D., Olsen, J.E., De Medici, D., 2014. European validation of a real-time PCR-based method for detection of *Listeria monocytogenes* in soft cheese. International Journal of Food Microbiology 184, 128–133. https://doi.org/10.1016/j.ijfoodmicro.2013.12.021

Guo, L., Ye, L., Zhao, Q., Ma, Y., Yang, J., Luo, Y., 2014. Comparative study of MALDI-TOF MS and VITEK 2 in bacteria identification. Journal of Thoracic Disease 6, 534–538. https://doi.org/10.3978/j.issn.2072-1439.2014.02.18

Gupta, V.K., Yola, M.L., Qureshi, M.S., Qureshi, M.S., 2013. A novel impedimetric biosensor based on graphene oxide/gold nanoplatform for detection of DNA arrays. Sensors and Actuators B: Chemical 188, 1201–1211. https://doi.org/10.1016/j.snb.2013.08.034

Hoelzer, K., Chen, Y., Dennis, S., Evans, P., Pouillot, R., Silk, B.J., Walls, I., 2013. New data, strategies, and insights for *Listeria monocytogenes* dose-response models. Risk Analysis 33, 1568–1581. https://doi.org/10.1111/risa.12005

Inės, A., Cosme, F., 2025. Biosensors for detecting food contaminants—an overview. Processes 13, 380. https://doi.org/10.3390/pr13020380

James, O.K., Wuni, A., Akabanda, F., Jespersen, L., 2018. Prevalence and characteristics of *Listeria monocytogenes* isolates in raw milk, heated milk and Nunu, a spontaneously fermented milk beverage, in Ghana. Beverages 4, 20. https://doi.org/10.3390/beverages4020040

Jia, S., Ma, A., Dong, H., Xia, S., 2022. Quantifiable effect of interparticle plasmonic coupling on sensitivity and tuning range for wavelength-mode LSPR fiber sensor fabricated by simple immobilization method. Sensors 22, 9075. https://doi.org/10.3390/s22239075

Kahraman, T., Ozmen, G., Ozinan, B., Göksoy, E., 2010. Prevalence of *Salmonella* spp. and *Listeria monocytogenes* in different cheese types produced in Turkey. British Food Journal 112, 1230–1236. https://doi.org/10.1108/00070701011088214

Karnwal, A., Sachan, R.S.K., Devgon, I., Devgon, J., Pant, G., Panchpuri, M., Ahmad, A., Alshammari, M.B., Hossain, K., Kumar, G., 2024. Gold nanoparticles in nanobiotechnology: from synthesis to biosensing applications. ACS Omega 9, 29966–29982. https://doi.org/10.1021/acsomega.3c10352

Kayode, A., Okoh, A., 2022. Assessment of multidrug-resistant *Listeria monocytogenes* in milk and milk products and One Health perspective. PLoS ONE 17, 1–21. https://doi.org/10.1371/journal.pone

Laximan, S., Kaur, S., Aulakh, R.S., Gill, J.P.S., 2016. Molecular characterization of *Listeria monocytogenes* in bovine milk and evaluating the sensitivity of PCR for direct detection in milk. The Indian Journal of Animal Sciences 86(5). https://doi.org/10.56093/ijans.v86i5.58443

Li, Y., Gan, Z., Zhou, X., Chen, Z., 2022. Accurate classification of *Listeria* species by MALDI-TOF mass spectrometry incorporating denoising autoencoder and machine learning. Journal of Microbiological Methods 192, 106378. https://doi.org/10.1016/j.mimet.2021.106378

Lin, Y.-H., Chen, S.-H., Chuang, Y.-C., Lu, Y.-C., Shen, T.Y., Chang, C.A., Lin, C.-S., 2008. Disposable amperometric immunosensing strips fabricated by Au nanoparticles-modified screen-printed carbon electrodes for the detection of foodborne pathogen *Escherichia coli* O157:H7. Biosensors and Bioelectronics 23, 1832–1837. https://doi.org/10.1016/j.bios.2008.02.030

Liu, D., Lawrence, M.L., Ainsworth, A.J., Austin, F.W., 2005. Comparative assessment of acid, alkali and salt tolerance in *Listeria monocytogenes* virulent and avirulent strains. FEMS Microbiology Letters 243, 373–378. https://doi.org/10.1016/j.femsle.2004.12.025

Mocan, T., Matea, C.T., Pop, T., Mosteanu, O., Buzoianu, A.D., Puia, C., Iancu, C., Mocan, L., 2017. Development of nanoparticle-based optical sensors for pathogenic bacterial detection. Journal of Nanobiotechnology 15, 25. https://doi.org/10.1186/s12951-017-0260-y

Moosavy, M.-H., Esmaeili, S., Mostafavi, E., Bagheri Amiri, F., 2014. Isolation of *Listeria monocytogenes* from milks used for Iranian traditional cheese in Lighvan cheese factories. Annals of Agricultural and Environmental Medicine 21(4), 728–729. https://doi.org/10.5604/12321966.1129923

Osek, J., Lachtara, B., Wieczorek, K., 2022. *Listeria monocytogenes* - How This Pathogen Survives in Food-Production Environments? Front Microbiol. 13, 866462.

Park, S.H., You, Y., 2023. Gold nanoparticle-based colorimetric biosensing for foodborne pathogen detection. Foods 13, 95. https://doi.org/10.3390/foods13010095

Pyz-Łukasik, R., Gondek, M., Winiarczyk, D., Michalak, K., Paszkiewicz, W., Piróg-Komorowska, A., Policht, A. and Ziomek, M., 2021. Occurrence of *Listeria monocytogenes* in artisanal cheeses from Poland and its identification by MALDI-TOF MS. Pathogens 10, 632. https://doi.org/10.3390/pathogens10060632

Quintela, I.A., de Los Reyes, B.G., Lin, C.S., Wu, V.C.H., 2019. Simultaneous colorimetric detection of *Salmonella* spp. in food and environmental samples by optical biosensing using oligonucleotide-gold nanoparticles. Frontiers in Microbiology 10, 1138. https://doi.org/10.3389/fmicb.2019.01138

Rezaei, M., Khomeiri, M., Ebrahimi, M., Kiani, S., Raeisi, M., 2019. Biochemical and molecular identification of *Listeria monocytogenes* and *Escherichia coli* in the raw milk samples delivered to the dairy farms in Golestan Province, Iran. Journal of Human, Environment, and Health Promotion 5, 160–164. https://doi.org/10.29252/jhehp.5.4.3

Roberts, D., Greenwood, M., 2003. Practical food microbiology. Blackwell Publishing, Oxford, USA.

Saleh, E., Elboudy, A., Elsayed, A., Ali, E., 2021. Molecular characterization of *Listeria monocytogenes* isolated from raw milk and some dairy products at local markets in Damanhour City, Egypt. Damanhour Journal of Veterinary Sciences 6, 1–6. https://doi.org/10.21608/djvs.2021.187849

Soni, D.K., Ahmad, R., Dubey, S.K., 2018. Biosensor for the detection of *Listeria monocytogenes*: emerging trends. Critical Reviews in Microbiology 44, 590–608. https://doi.org/10.1080/1040841X.2018.1473331

Tahoun, A.B.M.B., Abou Elez, R.M.M., Abdelfatah, E.N., Elsohaby, I., El-Gedawy, A.A., Elmoslemany, A.M., 2017. *Listeria monocytogenes* in raw milk, milking equipment and dairy workers: molecular characterization and antimicrobial resistance patterns. Journal of Global Antimicrobial Resistance 10, 264–270. https://doi.org/10.1016/j.jgar.2017.07.008

Tirkey, A., Babu, P.J., 2024. Synthesis and characterization of citrate-capped gold nanoparticles and their application in selective detection of creatinine (a kidney biomarker). Sensors International 5, 100252. https://doi.org/10.1016/j.sintl.2023.100252

Wachiralurpan, S., Sriyapai, T., Areekit, S., Sriyapai, P., Augkarawaritsawong, S., Santiwatanakul, S., Chansiri, K., 2018. Rapid colorimetric assay for detection of *Listeria monocytogenes* in food samples using LAMP formation of DNA concatemers and gold nanoparticle-DNA probe complex. Frontiers in Chemistry 6, 90. https://doi.org/10.3389/fchem.2018.00090

Xiao, Y., Zhang, Z., Yin, S., Ma, X., 2023. Nanoplasmonic biosensors for precision medicine. Frontiers in Chemistry 11. https://doi.org/10.3389/fchem.2023.1209744

Yola, M.L., Atar, N., 2014. A novel voltammetric sensor based on gold nanoparticles involved in p-aminothiophenol functionalized multi-walled carbon nanotubes: application to the simultaneous determination of quercetin and rutin. Electrochimica Acta 119, 24–31. https://doi.org/10.1016/j.electacta.2013.12.028

Zhang, Y., Wang, Y., Zhu, W., Wang, J., Yue, X., Liu, W., Zhang, D., Wang, J., 2017. Simultaneous colorimetric determination of bisphenol A and bisphenol S via a multi-level DNA circuit mediated by aptamers and gold nanoparticles. Microchimica Acta 184, 951–959. https://doi.org/10.1007/s00604-017-2092-8

Zhu, X., Chen, Y., Feng, C., Wang, W., Bo, B., Ren, R., Li, G., 2017. Assembly of self-cleaning electrode surface for the development of refreshable biosensors. Analytical Chemistry 89, 4131–4138. https://doi.org/10.1021/acs.analchem.6b05177